



Oil-palm and Rainforest Phytoliths Dissolve at Different Rates - with Implications for Silicon Cycling After Transformation of Rainforest Into Oil-palm Plantation

Barbara von der Lüche^{1,2} · Karin Bezler¹ · Harold J. Hughes¹ · Britta Greenshields¹ · Aiyen Tjoa³ · Daniela Sauer¹

Received: 16 June 2022 / Accepted: 14 August 2022 / Published online: 17 September 2022
© Springer Nature B.V. 2022, corrected publication 2022

Abstract

Phytoliths make up the predominant fraction of biogenic silica in plant litter and soils. Thus, they represent a major source of dissolved silicon (Si) in soil-plant systems. Dissolution of phytoliths from Si-accumulating crops such as rice has been well studied in recent years. However, phytolith dissolution in oil-palm plantations remains largely understudied. In this study, we compared dissolution rates of phytoliths isolated from oil-palm fronds, oil-palm litter, and rainforest litter. Our results showed that phytoliths from oil-palm fronds represent an important reservoir of easily dissolvable Si with high dissolution rates (0.44 - 0.69 mg g⁻¹ d⁻¹). Compared to fresh phytoliths from oil-palm fronds, phytoliths isolated from litter showed up to 18 times lower dissolution rates, reflecting silica aging over time. The dissolution rate of phytoliths isolated from rainforest litter (0.067 mg g⁻¹ d⁻¹) was significantly higher than that of phytoliths from oil-palm litter (0.038 mg g⁻¹ d⁻¹). These results demonstrate that transformation of rainforest into oil-palm plantation involves a major change in phytolith production and Si release from litter, considerably altering Si cycling in the soil-plant system. We identified cut-off palm fronds that are usually piled up between the palm rows as most important Si sources maintaining biogeochemical Si cycling in oil-palm plantations.

Keywords Land-use/land-cover transformation · Silicon · Oil-palm plantations · Phytolith · Silicon cycling · Dissolution · Biogenic silica · Rainforest

1 Introduction

Phytoliths are formed in plants through the uptake of dissolved monomeric silicic acid (H₄SiO₄) from soil solution and precipitation within cells, cell walls and intercellular spaces as small opal bodies (SiO₂ · nH₂O) [1, 2]. They are returned to soils through litterfall and decomposition, and contribute a major portion to the soils' biogenic silica (BSi) pool [3, 4]. Compared to most siliceous soil minerals, phytoliths are more soluble and constitute an important source

of plant-available silicon (Si) in the upper soil horizons [1, 3, 4].

Phytolith dissolution depends on various factors such as age, morphotype, surface area, surface roughness and condensation state of the silica [5–9]. In mixed flow reactors, the solubility product of phytoliths was similar among the analysed plant species, close to that of amorphous silica, but up to 10 times higher than that of quartz [7]. When normalising dissolution rates to phytolith mass rather than specific surface area (SSA), rates differ between plant species. It is for example ~ 30 times higher for horsetail (6.6E-06 mol g⁻¹ day⁻¹) than for pine needles (1.25E-08 mol g⁻¹ day⁻¹, 25°C, pH 6 ± 0.5) [6]. Besides phytoliths, plants may contain additional silica pools in form of individual H₄SiO₄ molecules or small polymers dispersed or complexed with the organic matrix [10]. Fraysse et al. 2006 [6] showed that Si release from the organic matrix of horsetail and pine needles was similar to that from phytolith dissolution. This suggests that the major part of Si is released from phytoliths. Yet, there is a considerable knowledge gap with respect to phytolith

✉ Barbara von der Lüche
barbara.von-der-luehe@uni-muenster.de

¹ Department of Physical Geography, University of Göttingen, Göttingen, Germany

² Present Address: Faculty of Geosciences, University of Münster, Münster, Germany

³ Department of Agrotechnology, Tadulako University, Palu, Indonesia

dissolution rates of plant litter, especially when the plant cover is altered by land-use/land-cover (LULC) changes.

It is widely assumed that the contribution of plants to Si dynamics in strongly weathered tropical soils is more important than in soils of temperate or boreal climates [11–14]. In natural tropical rainforests, phytoliths are an important Si source to maintain Si availability for plants [3, 4]. Transforming tropical rainforests into arable land may result in reduced Si supply to crops, especially, in soils that are strongly desilicated, thus having low levels of plant-available Si [15, 16]. In the long-term, LULC change may lead to increased losses of BSi from the soil system due to accelerated Si leaching, harvest and topsoil erosion [17–20].

In Indonesia, large areas of lowland rainforest have been converted to rubber and oil-palm plantations. Since the 1990s, oil palm has been the preferred cash crop [21]. Oil palms (*Elaeis guineensis*) are known to accumulate substantial quantities of Si (2.3 ± 0.7 wt.% [22]) in their above-ground biomass and are considered being Si-accumulating plants (= Si ≥ 1 wt. % [23]). Consequently, it is highly relevant to quantify phytolith dissolution from oil palms and evaluate its implications for Si cycling in soils, especially when oil palms replace former rainforest.

So far, little is known about the impact of oil-palm cultivation on Si fluxes and losses from tropical soils. Munevar and Romero (2015) [22] found lower quantities of plant-available Si in strongly weathered soils compared to less weathered soils. Si levels in 17 oil palm plantations in Colombia were generally higher. In the plant, they detected increasing Si concentrations with oil-palm frond age, indicating Si accumulation over time and immobile behaviour of Si [22]. Von der Lühe et al. (2020) [20] found trends of decreasing amorphous silica (ASi, which mainly consists of BSi in topsoils) in topsoils when lowland rainforests were converted to oil-palm plantations on Sumatra, Indonesia. In batch experiments, larger quantities of Si were released by oil-palm litter ($44 \pm 12 \mu\text{g Si g}^{-1}$ litter) compared to rainforest litter ($32 \pm 8 \mu\text{g Si g}^{-1}$ litter) after 28 h of continuous shaking. This was due to higher Si concentrations in the oil-palm litter ($23 \pm 5 \text{ mg g}^{-1}$, in rainforest litter: $13 \pm 2 \text{ mg g}^{-1}$) [20].

Conversion of lowland rainforest to oil-palm plantation causes changes in soil chemistry [24–28] and it is expected that Si fluxes and cycling in soils is affected as well, e.g. through increased Si uptake by oil palms and through topsoil erosion [20, 22]. Topsoil erosion greatly contributes to losses of nutrients and plant-available Si in oil-palm plantations [26, 29]. The return of sources of plant-available Si such as phytoliths is important for long-term Si supply, especially because oil palms are considered being Si accumulators [22]. In this study, we quantified the long-term steady-state dissolution of oil-palm phytoliths. We characterised differences between different ages of oil-palm phytoliths and compared them to the dissolution of phytoliths isolated

from lowland rainforest litter. Results are important for the quantification of Si cycling and availability of dissolved Si in tropical landscapes that have undergone transformation to oil-palm plantations.

2 Material and Methods

2.1 Study Area and Sampling Sites

The study area is located in Jambi Province ($^{\circ}155'40''$ S, $^{\circ}103'15'33''$ E, 70 ± 4 m above sea level) in south-west Sumatra, Indonesia [30]. The climate is humid-tropical with a mean annual precipitation of 2235 ± 381 mm and a mean annual temperature of 26.7 ± 0.2 °C (1991–2011) with two rainy seasons peaking in March and December and a dry season from June to September [30]. Acrisols dominate the study area. Soils typically have 1–2 % organic carbon in their topsoils, pH 4.5 and loamy texture with 21–54 % clay. The sampling sites (50 x 50 m plots) were established by the Collaborative Research Centre 990 [30] funded by the German Research Foundation (DFG). Samples were collected from three lowland rainforest sites (HF2 - 4) and three smallholder oil-palm plantation sites (HO2 - 4). The rainforest plots were located within the Harapan Rainforest, an area that is protected since 2007 to restore the ecosystem structure and its biodiversity [30]. The oil-palm plantations were established around 8 to 17 years ago and are subject to common smallholder-management practices [30]. Oil-palm plantations are typically managed in oil-palm rows with approximately 9 m between neighbouring trees within a row, separated by ca. 9 m wide interrows in between the oil-palm rows (Fig. 1). Fronds that are cut off oil-palm trees, are piled up in every second interrow (Fig. 1).

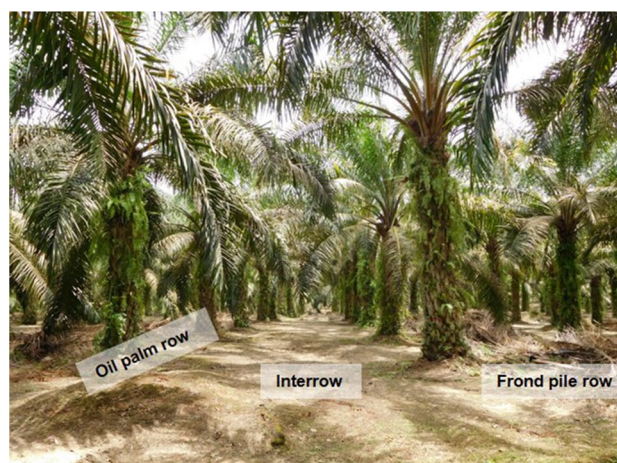


Fig. 1 Typical management of oil-palm plantations with oil-palm row, interrow and frond-pile row. Photo from HO3: Barbara von der Lühe, 2016

2.2 Sampling of Litter and Leaves

In each rainforest plot, three litter samples were collected in an area of 20 x 20 cm ($n = 3$). Under oil-palm plantations, litter was collected from frond piles, directly above the soil surface ($n = 3$). Oil-palm fronds were collected from three trees in the oil-palm plots (HO2 - 4). The litter was composed of dead plant material that showed initial decomposition and fragmentation. Leaflet samples were taken from leaf number 17 (leaf No. 17) and from the oldest hanging leaf (dead leaf) that was still attached to the oil-palm stem. The sampling of leaf No. 17 was based on the nomenclature applied to the arrangement of leaves of oil palms. The youngest open leaf is given the number “1” and the following leaves are numbered consecutively [22]. The samples were dried (24 h, 70 °C) and finely shredded by use of a plant mill.

2.3 Phytolith Extraction

Phytoliths were extracted from litter and oil-palm frond materials according to the dry ashing method by Parr et al. (2001) [31]. The material (0.5 - 5 g) was placed into crucibles and ashed in a muffle furnace at 500 °C for 6 h. The samples were transferred into 50 ml tubes, and 10 ml of 10 % HCl was added. The samples were then heated in a water bath at 70 °C for 20 min. The tubes were centrifuged at 3500 rpm for 5 min and the supernatant was discarded. Samples were washed twice with 40 ml of deionised water by centrifuging at 3500 rpm for 5 min and discarding the supernatant. Residual organic material was removed by adding 10 ml of 15 % H₂O₂ and heating at 70 °C in a water bath for 2 h. Samples were washed twice with 20 ml of deionised water and dried at 40 °C for 48 h.

The phytoliths isolated from litter samples contained small quantities of mineral particles which were removed by use of the method of Lombardo et al. (2016) [32]. The phytoliths were treated four times by adding 40 ml of 5% sodium hexametaphosphate (NaPO₃)₆ by placing the samples in an ultrasonic bath at 60 °C for 10 min, centrifuging at 1500 rpm for 3 min and removing the supernatant. The samples were washed twice with 20 ml of deionized water, and the phytoliths were extracted by density-separation using 15 ml of sodium polytungstate (SPT, Na₆H₂W₁₂O₄₀ x H₂O) at a density of 2.3 g ml⁻¹. The samples were shaken and centrifuged at 3000 rpm for 5 min. The phytoliths floating on top of the liquid were collected with a pipette. SPT separation was repeated until no phytoliths were visible at the surface of the SPT solution. The collected phytoliths were rinsed twice with deionised water and dried at 40 °C for 48 h.

2.4 Si Leaching from Phytoliths

Phytolith leaching was carried out in simulated rainwater. This simulated rainwater was used to mimic the conditions of rainwater in Indonesia [20]. Chemical characteristics of simulated rainwater corresponded to rainwater of Palembang, Sumatra [33], which contains 0.1 mg l⁻¹ NH₄⁺, 0.0005 mg l⁻¹ Ca²⁺, 0.05 mg l⁻¹ K⁺, 0.13 mg l⁻¹ Na⁺, 0.45 mg l⁻¹ NO₃⁻, 0.49 mg l⁻¹ SO₄²⁻ and 0.19 mg l⁻¹ Cl⁻. About 5 mg of phytoliths (precision of ± 0.01 mg) were placed into 120 ml plastic tubes, and 100 ml of simulated rainwater was added. This wide water:phytolith ratio allowed for keeping the solution far from chemical equilibrium, thus ensuring that Si precipitation was negligible compared to dissolution flux. In this way, we ensured that Si release into the solution remained mostly linear over time. The tubes were not shaken permanently but only for 1 min h⁻¹ for 71 days to avoid enhanced Si release through phytolith abrasion. This approach allowed us to attribute the observed Si release mainly to the dissolution process of the phytoliths at near-natural conditions, and to compare the dissolution behaviour of phytoliths from different land-cover units. We monitored pH of the sample solutions throughout the experiment. Solutions of rainforest litter had a pH of 5.3 ± 0.1, those of oil-palm litter had a pH of 5.5 ± 0.1, solutions of oil-palm leaf no. 17 had a pH of 5.4 ± 0.07, and those of the dead hanging leaf had a pH of 5.4 ± 0.05.

Si concentrations of the solutions were analysed each week. For Si analysis, the 120 ml tubes were taken from the shaker and placed on a table for 5 min to allow the phytoliths to sink to the bottom of the tube after this movement. An aliquot of 12.5 ml was removed and centrifuged at 3000 rpm for 5 min. From this sample, a 6.25 ml aliquot was used for Si analyses. Fresh simulated rainwater was added to the remaining 6.25 ml of the 12.5 ml aliquot. After shaking the sample, the aliquot was returned to the 120 ml tubes to keep the volume of 100 ml simulated rainwater constant over the entire leaching experiment. Si analysis was performed by use of the molybdenum-blue colorimetric method of Grasshoff (2009) [34]. Si concentrations were corrected for the dilution with 6.25 ml simulated rainwater and related to phytolith mass in mg g⁻¹. Dissolution rates were calculated from the slopes of the linear regressions of the increasing Si concentrations (mg g⁻¹ d⁻¹) over time. All data are presented as grand means (of three sampling points per plot and three plots per LULC type) with standard deviation (mean ± SD).

2.5 Specific Surface Area of Phytoliths

Specific surface area (SSA) was measured on phytoliths isolated from oil-palm leaves before they were subjected to the dissolution experiment. Phytoliths were dried at 105 °C over

night and degassed on a VacPrep 061 (Micromeritics, Norcross, GA, USA) at 105 °C for 2 h. SSA was determined via single-point N_2 adsorption at a relative pressure of 0.05 - 0.3 p/p_0 by use of a Gemini VII (Micromeritics). The mean SSA of black carbon standard reference material ($20.70 \pm 0.18 \text{ m}^2 \text{ g}^{-1}$, $n = 4$) was consistent with the reference value from the manufacturer ($21.14 \pm 0.75 \text{ m}^2 \text{ g}^{-1}$). It has been shown that SSA of phytoliths decreases with progressing dissolution during leaching/shaking experiments [7]. Thus, dissolution rates were mass normalized without considering the SSA.

2.6 Statistical Analyses

Differences between the amounts of phytoliths extracted from litter samples were tested by comparing log-transformed grand means (of three sampling points per plot and three plots per LULC type). Data was tested for normal distribution by the Kolmogorov Smirnov test and for homogeneity of variances by the Levene test. Differences between LULC types were tested by one-way analysis of variance (ANOVA) following a Tukey HSD post-hoc test.

A linear mixed effect (LME) model [35] with temporal autocorrelation structure assessed significant differences between Si dissolution over the time intervals. LULC effects on phytolith dissolution were tested including LULC type and time as fixed effect and plot-ID as random factor. Statistical analysis was conducted on the grand mean (of three sampling points per plot and three plots per LULC type).

Differences were considered significant at $p \leq 0.05$. Statistical analysis was performed with SPSS 26 and R 3.0.2.

3 Results

3.1 Phytoliths in Leaves and Litter

The amounts of phytoliths isolated from rainforest litter were generally lower than those obtained from oil-palm litter ($17.6 \pm 3.3 \text{ mg g}^{-1}$, Fig. 2).

The highest amounts of phytoliths were isolated from the dead leaves of oil palms, reaching $49.3 \pm 31.8 \text{ mg g}^{-1}$, while intermediate amounts were isolated from leaf No. 17. However, phytoliths isolated from the dead leaves of oil palms did not differ significantly from the amount of phytoliths isolated from leaf 17 ($15.6 \pm 12.4 \text{ mg g}^{-1}$)(Fig. 2).

3.2 Si Leaching from Phytoliths

The batch dissolution experiments showed that dissolution of all phytolith samples was constant and remained linear over the period of 71 days (Fig. 3). The dissolution curves differed significantly ($p \leq 0.05$) between the rainforest and oil-palm litters, no significant difference was observed

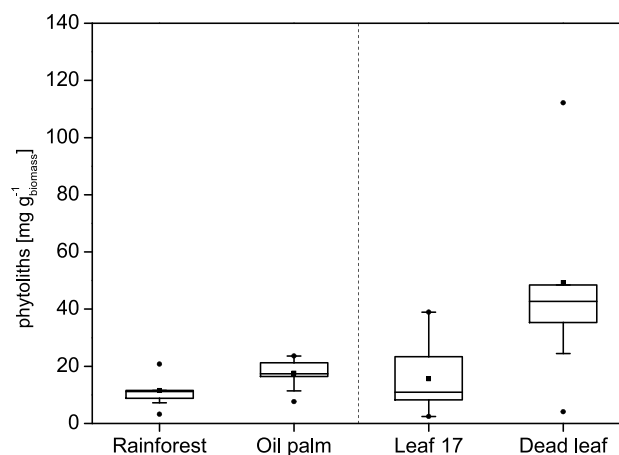


Fig. 2 Amounts of phytoliths in mg g^{-1} isolated from rainforest and oil-palm litter, and from leaf 17 and the dead hanging leaf of oil palms (grand means of three sampling points per plot and three plots per LULC type). Boxes indicate interquartile ranges and whiskers extend 1.5 times the interquartile range below or above the box. Statistical differences were tested between rainforest and oil-palm litter, and between leaf 17 and the dead leaf. No statistical differences (by ANOVA) were found between rainforest and oil-palm litter, and between leaf 17 and the dead leaf

between the dissolution curves of leaf 17 and the dead leaf (Fig. 3). The dissolution rate of phytoliths isolated from rainforest litter was $0.067 \pm 0.005 \text{ mg g}^{-1} \text{ d}^{-1}$ and was significantly higher ($p \leq 0.05$) than the dissolution rate of phytoliths isolated from oil-palm litter ($0.038 \pm 0.007 \text{ mg g}^{-1} \text{ d}^{-1}$, Fig. 3, Table 1).

The dissolution rates of phytoliths isolated from leaf No. 17 and from the dead leaf were remarkably higher compared to the dissolution rates of phytoliths isolated from litter (Fig. 3, Table 1). The dissolution rate of phytoliths isolated from the dead leaf was one order of magnitude higher than that of rainforest phytoliths and 17 times higher than that of oil-palm litter.

SSA of the phytoliths extracted from the dead leaf ($159.14 \pm 15.94 \text{ cm}^3 \text{ g}^{-1}$) was on average three times larger than that of the phytoliths of leaf No. 17 ($54.82 \pm 14.75 \text{ cm}^3 \text{ g}^{-1}$, Table 1). The difference was significant ($p \leq 0.05$). Dissolution rate increased with increasing SSA (Fig. 4), but no clear linear correlation was detected between SSA and dissolution rate, neither for phytoliths isolated from leaf 17 nor for those of the dead leaf.

4 Discussion

We observed the highest phytolith concentrations in the hanging dead leaves of the oil palms. This pattern reflects proceeding phytolith formation with increasing leaf age, and

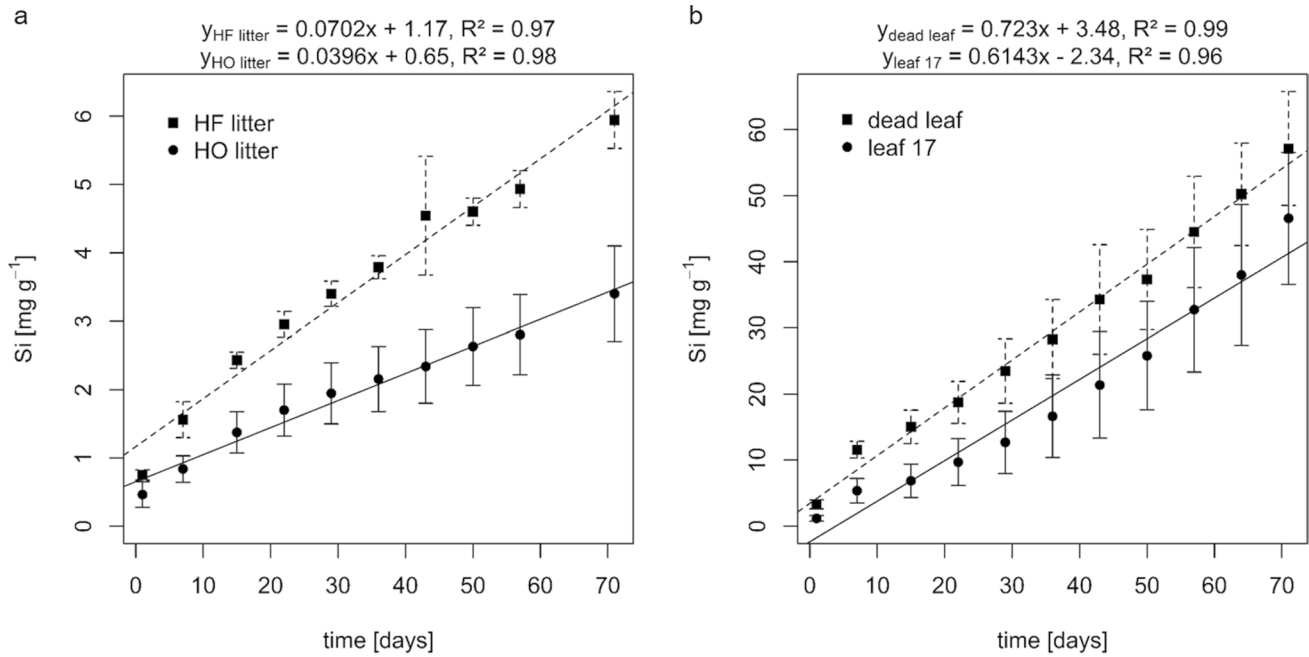


Fig. 3 Dissolution [mg g^{-1}] of phytoliths isolated from (a) lowland rainforest (HF) litter and oil-palm (HO) litter, and (b) oil-palm leaves

(leaf No. 17, dead leaf) in simulated rainwater. Data points represent grand means \pm standard deviation of three sampling points per plot and three plots per LULC type

Table 1 Si contents [wt. %], dissolution rates [$\text{mg g}^{-1} \text{d}^{-1}$] and specific surface area (SSA) [$\text{m}^2 \text{g}^{-1}$] of phytoliths isolated from rainforest and oil-palm litter, and from oil-palm leaflets of leaf No. 17 and the dead hanging leaf. Data are presented as grand means \pm standard deviation of phytoliths from three sampling points per plot and three plots per LULC type (HF 2 - 4, HO 2 - 4). Si contents in litter have been published earlier [20]

	Si [wt. %]	Dissolution rate [$\text{mg g}^{-1} \text{d}^{-1}$]	SSA [$\text{m}^2 \text{g}^{-1}$]
rainforest litter	1.3 ± 0.2	0.067 ± 0.005	-
oil palm litter	2.3 ± 0.5	0.038 ± 0.007	-
leaf No. 17	1.8 ± 0.7	0.44 ± 0.28	54.82 ± 14.75
dead leaf	3.6 ± 0.8	0.69 ± 0.16	159.14 ± 15.94

subsequent progressive dissolution of phytoliths in litter. A decrease in the amount of phytoliths in plant litter and soils has been observed in previous studies and has been associated to advancing phytolith dissolution [8, 9, 36, 37]. The stage of phytolith dissolution in litter depends on the age of the litter. In oil-palm plantations, frond piles remain in the same location over the entire life time of an oil-palm generation. Dead fronds are regularly cut off and piled up in rows. Thus, the age of the phytoliths might be younger or the same age of the studied oil-palm plantations (7 - 16 years).

We found that SSA of phytoliths isolated from leaf No. 17 and from the dead leaf differed significantly, showing increasing SSA with leaf age. Munevar and Romero (2015)

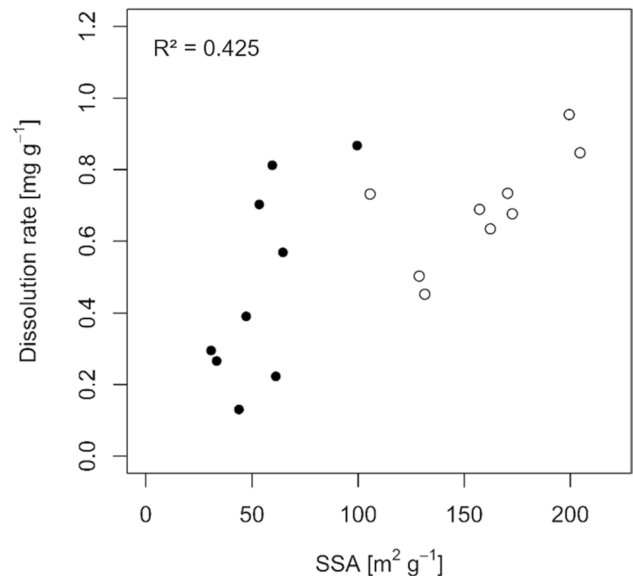


Fig. 4 Correlation between dissolution rate [$\text{mg g}^{-1} \text{d}^{-1}$] and SSA [$\text{m}^2 \text{g}^{-1}$] of phytoliths isolated from oil-palm leaf No. 17 (black circles, $n = 9$) and the dead leaf (open circles, $n = 9$)

[22] detected increasing Si concentrations in oil-palm leaves from leaf No. 1 (around 1.3 %) to leaf No. 25 (around 4 %) demonstrating that Si accumulates with leaf age. Silica precipitates within the cell walls, cell lumen and intercellular spaces of leaves. Silicic acid that is taken up by plants, is

mainly deposited in leaves, near stomata, where transpiration occurs. After precipitation, the silica behaves immobile in plant tissue [38], which results in the observed Si accumulation with leaf age. Our results suggest that SSA of the phytoliths increases with leaf age, too. One possible explanation for this increase could be that phytolith formation in younger leaves starts with more compact silica precipitates, and that advancing silica accumulation leads to more and more detailed pseudomorphosis of the phytoliths according to the cell structures that are progressively filled with silica. The more completely filigree cell structures are filled with silica over time, the larger should be the SSA of the phytoliths. SSA of the phytoliths of leaf No. 17 and of the dead leaf was in the same range as that of phytoliths of other plant species such as horsetail ($92.8 \text{ m}^2 \text{ g}^{-1}$), larch ($195.4 \text{ m}^2 \text{ g}^{-1}$), elm ($121.0 \text{ m}^2 \text{ g}^{-1}$), New Zealand tree fern ($315.9 \text{ m}^2 \text{ g}^{-1}$), bamboo (*Nastus borbonicus*, $159.5 \text{ m}^2 \text{ g}^{-1}$) and rice ($29.6 \text{ m}^2 \text{ g}^{-1}$) [6, 7, 37, 39] (Table 1).

Phytolith dissolution rates during our batch experiment might have been increased compared to natural conditions, because we had isolated the phytoliths by ashing the plant material at $500 \text{ }^\circ\text{C}$ for 6 h. Phytolith dissolution is influenced by sample pretreatment and by pH of the solution used for leaching experiments. Trinh et al. 2017 [39] reported differences in the solubility of phytoliths obtained from rice straw that had been ashed at different temperatures. They observed the highest solubility of phytoliths isolated from rice-straw that was ashed at $600 \text{ }^\circ\text{C}$. Above $700 \text{ }^\circ\text{C}$ silica crystallisation takes place, which could result in decreased dissolution rates [39]. Fraysse et al. (2006) [6] showed that phytolith-dissolution rates exhibit a minimum at pH 3. Thus, phytoliths might be better preserved in strongly acidic topsoils. Fraysse et al. (2009) [7] reported that within the typical natural soil pH range of pH 4–8, phytolith-dissolution rates were similar for all types of phytoliths from different plant species they analysed. Within this pH range, dissolution rates of phytoliths are 2–4 orders of magnitude above those of the main soil and rock minerals. In our experiment, we cannot exclude an influence of the high temperature to which our samples were subjected. Nevertheless, we consider the outcomes of our comparative study of dissolution rates of phytoliths isolated from different materials robust, because all samples were ashed at the same temperature and treated with simulated rainwater at pH 5.3–5.5.

In our study, all phytoliths isolated from rainforest litter, oil-palm litter, and leaves, steadily dissolved over 71 days. The highest dissolution rates were obtained for the phytoliths isolated from leaf No. 17 and from the dead leaf. Dissolution rates decreased with phytolith ageing as shown by the lower phytolith-dissolution rate of oil-palm litter. Overall, the solubility of phytoliths isolated from oil-palm litter ($1.4 \pm 0.3 \text{ } \mu\text{mol l}^{-1}$), leaf No. 17 ($16.4 \pm 10.1 \text{ } \mu\text{mol l}^{-1}$), and the dead leaf ($24.6 \pm 5.6 \text{ } \mu\text{mol l}^{-1}$) was in the same order of magnitude

as the solubility of phytoliths obtained from horsetail, which was $6.6 \text{ } \mu\text{mol g}^{-1} \text{ d}^{-1}$ ($25 \text{ }^\circ\text{C}$, pH 6 ± 0.5) [6].

Once introduced into topsoils, a major portion of the phytoliths is rapidly recycled, and only a little portion remains in the soils [3, 9, 40]. In a rainforest in Congo, Alexandre et al. (1997) [3] found that 92 % of the biogenic silica input into soils was rapidly recycled, while 8 % of the biogenic silica remained more stable. These results are in agreement with conclusions from other studies showing that dissolution rates of phytoliths in soils decrease with phytolith ageing [9, 40]. The results of our leaching experiment are also in line with these previous studies, since we found decreased dissolution rates for phytoliths isolated from litter, for which a certain stage of ageing can be assumed, compared to fresh phytoliths obtained from leaves. Another reason for decreasing phytolith-dissolution rates in litter over time is that fresh phytoliths still include a considerable portion of filigree parts, according to the plant-cell structures, along which the silica precipitated, and consequently have much higher SSA than older, partially dissolved and, thereby, progressively rounded phytoliths [37].

Our experiment yielded higher dissolution rates for phytoliths isolated from rainforest litter compared to those of phytoliths obtained from oil-palm litter. Leaves of different tree species in a tropical rainforest differ considerably with respect to their Si concentrations (0–12.6 wt. %) [14, 41, 42], and rainforest litter includes a great variety of phytoliths from different plant species. These phytoliths have differing size and shape, they have been formed over differing time-spans in the living leaves of plants, and they have been subject to ageing for differing time-spans after litterfall [43]. With this diversity in phytolith shape, size and age, the average phytolith-dissolution rate of rainforest litter is about twice the phytolith-dissolution rate of oil-palm litter (Fig. 3). The observed larger SSA and higher dissolution rates of phytoliths from the hanging dead leaf compared to those of leaf No. 17 (Fig. 4) suggested that both SSA and dissolution rate of oil-palm phytoliths increase with leaf age. The relationship between SSA and dissolution rate showed considerable data scatter, demonstrating that other factors such as surface properties, phytolith morphology, surface roughness, and condensation state also affect phytolith-dissolution rates [44]. Cabanes and Shahack-Gross (2015) [45] hypothesized phytolith morphotypes to be more important for the phytolith-dissolution rate than nanoscopic SSA of phytoliths.

5 Conclusion

This study revealed differences in phytolith concentrations and dissolution rates between tropical lowland rainforest and oil-palm plantations that have relevant implications for ecosystem silicon cycling. Phytoliths, representing the major

fraction of BSi in soils, were slightly more abundant in oil-palm fronds and oil-palm litter than in rainforest litter. This difference can be explained by enhanced Si accumulation in oil-palm fronds. Phytoliths isolated from oil-palm fronds (leaf 17, hanging dead leaf) moreover exhibited high dissolution rates. Aged phytoliths obtained from oil-palm litter showed lower dissolution rates. Their dissolution rates were also lower than those of phytoliths isolated from rainforest litter. These outcomes of our study imply that dissolution of the high amounts of rapidly dissolving fresh phytoliths in dead oil-palm fronds may ensure the replenishment of plant-available Si in soils under frond-pile rows in oil-palm plantations. Thus, phytoliths represent a key factor to maintain Si cycling in oil-palm plantations and long-term Si supply to oil palms after rainforest transformation. However, a final evaluation of the long-term effect of oil-palm cultivation on Si cycling requires consideration of all Si fluxes such as Si losses from the system through harvest. These fluxes also depend on management practices, including the degree of topsoil disruption in the course of plantation establishment, Si losses via topsoil erosion, and possible return of empty fruit bunches to the system.

Acknowledgements We thank the Indonesian Ministry of Research, Technology and Higher Education (RISTEKDIKTI), the Indonesian Institute of Sciences (LIPI) and the Ministry of Forestry (PHKA) for research permission in Indonesia. Litter and leaf sampling were conducted using the research permit 110 / SIP / FRP / E5 / Dit.KI / IV / 2018 and 187 / E5 / E5.4 / SIP / 2019. The authors wish to thank our local field assistants in Indonesia Nando, Somat, Daniel and Sofian, as well as Megawati and Yuding for their great support, and PT REKI for providing access to the rainforest research plots. We thank Dr. Jürgen Grotheer, Petra Voigt, Anja Södje and Angelika Mroncz for their valuable help in the laboratory.

Author Contributions Barbara von der Lüche, Karin Bezler, Harold J. Hughes, Aiyen Tjoa and Daniela Sauer contributed to the study conception and design. Field work was conducted by Britta Greenshields, Daniela Sauer and Barbara von der Lüche. Material preparation, data collection and analysis were performed by Barbara von der Lüche and Karin Bezler. The first draft of the manuscript was written by Barbara von der Lüche and all authors commented on previous versions of the manuscript. All authors read and approved the final manuscript.

Funding Open Access funding enabled and organized by Projekt DEAL. This project (project no. 391702217) was funded by the German Research Foundation (DFG) and was associated to the DFG Collaborative Research Centre 990 (project no. 192626868; <http://www.uni-goettingen.de/crc990>).

Availability of data and material The datasets generated during and/or analysed during the current study are available from the corresponding author on reasonable request.

Declarations

Conflicts of interest The authors have no relevant financial or non-financial interests to disclose.

Open Access This article is licensed under a Creative Commons Attribution 4.0 International License, which permits use, sharing, adaptation, distribution and reproduction in any medium or format, as long as you give appropriate credit to the original author(s) and the source, provide a link to the Creative Commons licence, and indicate if changes were made. The images or other third party material in this article are included in the article's Creative Commons licence, unless indicated otherwise in a credit line to the material. If material is not included in the article's Creative Commons licence and your intended use is not permitted by statutory regulation or exceeds the permitted use, you will need to obtain permission directly from the copyright holder. To view a copy of this licence, visit <http://creativecommons.org/licenses/by/4.0/>.

References

- Lucas Y (2001) *Annu Rev Earth Planet Sci* 29(1):135–163. <https://doi.org/10.1146/annurev.earth.29.1.135>
- Piperno DR, (2006) Phytoliths: a comprehensive guide for archaeologists and paleoecologists. Lanham, Altamira
- Alexandre A, Meunier JD, Colin F, Koud JM (1997) *Geochim Cosmochim Acta* 61(3):677–682. [https://doi.org/10.1016/S0016-7037\(97\)00001-X](https://doi.org/10.1016/S0016-7037(97)00001-X)
- Meunier JD, Colin F, Alarcon C (1999) *Geology* 27(9):835–838. [https://doi.org/10.1130/0091-7613\(1999\)027<0835:BSSIS>2.3.CO;2](https://doi.org/10.1130/0091-7613(1999)027<0835:BSSIS>2.3.CO;2)
- Albert RM, Bamford MK, Cabanes D (2006) *Quat Int* 148(1):78–94. <https://doi.org/10.1016/j.quaint.2005.11.026>
- Frayse F, Cantais F, Pokrovsky OS, Schott J, Meunier JD (2006) *J Geochem Explor* 88(1–3):202–205. <https://doi.org/10.1016/j.gexplo.2005.08.039>
- Frayse F, Pokrovsky OS, Schott J, Meunier JD (2009) *Chem Geology* 258(3–4):197–206. <https://doi.org/10.1016/j.chemgeo.2008.10.003>
- Cabanes D, Weiner S, Shahack-Gross R (2011) *J Archaeol Sci* 38(9):2480–2490. <https://doi.org/10.1016/j.jas.2011.05.020>
- Meunier JD, Keller C, Guntzer F, Riotte J, Braun JJ, Anupama K (2014) *Geoderma* 216:30–35. <https://doi.org/10.1016/j.geoderma.2013.10.014>
- Frayse F, Pokrovsky O, Meunier JD (2010) *Geochim Cosmochim Acta* 74(1):70–84. <https://doi.org/10.1016/j.gca.2009.09.002>
- Lucas Y, Luizão FJ, Chauvel A, Rouiller J, Nahon D (1993) *Science* 260(5107):521–523. <https://doi.org/10.1126/science.260.5107.521>
- Pokrovsky O, Schott J, Kudryavtzev D, Dupré B (2005) *Geochim Cosmochim Acta* 69(24):5659–5680. <https://doi.org/10.1016/j.gca.2005.07.018>
- Zakharova E, Pokrovsky OS, Dupré B, Gaillardet J, Efimova L (2007) *Chem Geol* 242(1–2):255–277. <https://doi.org/10.1016/j.chemgeo.2007.03.018>
- Nakamura R, Ishizawa H, Wagai R, Suzuki S, Kitayama K, Kitajima K, (2019) *Plant Soil* 443:155–166. <https://doi.org/10.1007/s11104-019-04230-7>
- Meunier JD, Sandhya K, Prakash NB, Borschneck D, Dussouillez P (2018) *Plant Soil* 432(1):143–155. <https://doi.org/10.1007/s11104-018-3758-7>
- De Tombeur F, Vander Linden C, Cornélis JT, Godin B, Compère P, Delvaux B (2020) *Plant Soil* 452(1):529–546. <https://doi.org/10.1007/s11104-020-04588-z>
- Unzué-Belmonte D, Ameijeiras-Mariño Y, Opfergelt S, Cornelis JT, Barão L, Minella J, Meire P, Struyf E (2017) *Solid Earth* 8(4):737–750. <https://doi.org/10.5194/se-8-737-2017>
- Conley DJ, Likens GE, Buso DC, Saccone L, Bailey SW, Johnson CE (2008) *Glob Change Biol* 14(11):2548–2554. <https://doi.org/10.1111/j.1365-2486.2008.01667.x>

19. Struyf E, Smis A, Van Damme S, Garnier J, Govers G, Van Wesemael B, Conley DJ, Batelaan O, Frot E, Clymans W, Vandevenne F, Lancelot C, Goos P, Meire P (2010) *Nat Commun* 1:129. <https://doi.org/10.1038/ncomms1128>
20. Von der Lühe B, Pauli L, Greenshields B, Hughes HJ, Tjoa A, Sauer D, (2020) *Silicon* 13:4345–4353. <https://doi.org/10.1007/s12633-020-00680-2>
21. Margono BA, Turubanova S, Zhuravleva I, Potapov P, Tyukavina A, Baccini A, Goetz S, Hansen MC (2012) *Environ Res Lett* 7(3):034010. <https://doi.org/10.1088/1748-9326/7/3/034010>
22. Munevar F, Romero A (2015) *Exp Agr* 51(3):382–392. <https://doi.org/10.1017/S0014479714000374>
23. Ma JF, Miyake Y, Takahashi E, (2001) In: Datnoff LE, Snyder GH, Korndörfer GH (eds) *Silicon in Agriculture*. Elsevier, Amsterdam, pp. 17–39. [https://doi.org/10.1016/S0928-3420\(01\)80006-9](https://doi.org/10.1016/S0928-3420(01)80006-9)
24. Allen K, Corre MD, Tjoa A, Veldkamp E (2015) *PloS One* 10(7):e0133325. <https://doi.org/10.1371/journal.pone.0133325>
25. Allen K, Corre MD, Kurniawan S, Utami SR, Veldkamp E (2016) *Geoderma* 284:42–50. <https://doi.org/10.1016/j.geoderma.2016.08.010>
26. Guillaume T, Damris M, Kuzyakov Y (2015) *Glob Change Biol* 21(9):3548–3560. <https://doi.org/10.1111/gcb.12907>
27. Guillaume T, Holtkamp AM, Damris M, Brümmer B, Kuzyakov Y (2016) *Agriculture, Ecosystems & Environment* 232:110–118. <https://doi.org/10.1016/j.agee.2016.07.002>
28. Hennings N, Becker JN, Guillaume T, Damris M, Dippold MA, Kuzyakov Y (2021) *Catena* 196:104941. <https://doi.org/10.1016/j.catena.2020.104941>
29. Dislich C, Keyel AC, Salecker J, Kisel Y, Meyer KM, Auliya M, Barnes AD, Corre MD, Darras K, Faust H, Hess B, Klasen S, Knohl A, Kreft H, Mejjide A, Nurdiansyah F, Otten F, Pe'er G, Steinebach S, Tarigan S, Tölle MH, Tschardt T, Wiegand K (2017) *Biol Rev* 92(3):1539–1569. <https://doi.org/10.1111/brv.12295>
30. Drescher J, Rembold K, Allen K, Beckschäfer P, Buchori D, Clough Y, Faust H, Fauzi AM, Gunawan D, Hertel D, Irawan B, Jaya INS, Klarner B, Kleinn C, Knohl A, Kotowska MM, Krashchanska V, Krishna V, Leuschner C, Lorenz W, Mejjide A, Melati D, Nomura M, Pérez-Cruzado C, Qaim M, Siregar IZ, Steinebach S, Tjoa A, Tschardt T, Wick B, Wiegand K, Kreft H, Scheu S (2016) *Philosophical Transactions of the Royal Society B: Biological Sciences* 371(1694):20150275. <https://doi.org/10.1098/rstb.2015.0275>
31. Parr JF, Lentfer CJ, Boyd WE (2001) *J Archaeol Sci* 28(8):875–886. <https://doi.org/10.1006/jasc.2000.0623>
32. Lombardo U, Ruiz-Pérez J, Madella M (2016) *Rev Palaeobot Palynol* 235:1–5. <https://doi.org/10.1016/j.revpalbo.2016.09.008>
33. Budiwati T, Setyawati W, Aries Tanti D, (2016) *Int J Atmos Sci* 1876046:1–11. <https://doi.org/10.1155/2016/1876046>
34. Grasshoff K, Kremling K, Ehrhardt M, 2009 *Methods of seawater analysis*. Wiley, Weinheim
35. Crawley MJ, 2012 *The R book*. Wiley, Weinheim
36. Drees LR, Wilding LP, Smeck NE, Senkayi AL (1977) In: Dixon JB and Weed SB (eds) *Minerals in Soil Environments*. Soil Science Society of America, Madison
37. Frayse F, Pokrovsky OS, Schott J, Meunier JD (2006) *Geochim Cosmochim Acta* 70(8):1939–1951. <https://doi.org/10.1016/j.gca.2005.12.025>
38. Epstein E (1994) *Proc Natl Acad Sci* 91(1):11–17. <https://doi.org/10.1073/pnas.91.1.11>
39. Trinh TK, Nguyen TT, Nguyen TN, Wu TY, Meharg AA, Nguyen MN (2017) *Soil Till Res* 171:19–24. <https://doi.org/10.1016/j.still.2017.04.002>
40. Barão L, Clymans W, Vandevenne F, Meire P, Conley D, Struyf E (2014) *Eur J Soil Sci* 65(5):693–705. <https://doi.org/10.1111/ejss.12161>
41. Ishizawa H, Niiyama K, Tida Y, Shari NH, Ripin A, Kitajima K (2019) *Ecolog Res* 34(4):548–559. <https://doi.org/10.1111/1440-1703.1202>
42. Nakamura R, Cornelis JT, De Tombeur F, Yoshinaga A, Nakagawa M, Kitajima K (2020) *Geoderma* 368:114288. <https://doi.org/10.1016/j.geoderma.2020.114288>
43. Bartoli F, Wilding L (1980) *Soil Sci Soc Am J* 44(4):873–878. <https://doi.org/10.2136/sssaj1980.03615995004400040043x>
44. Bartoli F (1985) *Eur J Soil Sci* 36(3):335–350. <https://doi.org/10.1111/j.1365-2389.1985.tb00340.x>
45. Cabanes D, Shahack-Gross R (2015) *PloS one* 10(5):e0125532. <https://doi.org/10.1371/journal.pone.0125532>

Publisher's Note Springer Nature remains neutral with regard to jurisdictional claims in published maps and institutional affiliations.